region Pb-Po. For the nuclear radius parameter $r_0=1.2\times10^{-13}$ cm and $\Gamma=-0.1$, Strutinskii calculates $(Z^2/A)_{\text{crit}}\approx43$-47. This value compares favorably with the values deduced above as extrapolations of the best fits for experimentally measured saddle deformations in the heavy-element region. This agreement lends further support to the validity of the modified liquid-drop model of the nucleus, which allows for the surface tension to vary with the curvature of the nuclear surface.

ACKNOWLEDGMENTS

The authors are indebted to J. Milsted for the supply and preparation of the Cf^{249} source, and to J. Munro for technical assistance in the preparation of target backing, and for fabrication of the semiconductor detectors. Several of the transneptunium nuclides were kindly supplied by H. Diamond and D. Cohen of the Heavy Element Group to whom we are also indebted for advice on heavy-element purification.

PHYSICAL REVIEW VOLUME 141, NUMBER 3 JANUARY 1966

Isobaric Analogue States in Heavy Nuclei. I. Molybdenum Isotopes*

C. F. Moore,† P. Richard,‡ C. E. Watson,§ D. Robson, and J. D. Fox
Department of Physics, Florida State University, Tallahassee, Florida
(Received 28 June 1965)

Isobaric analogue states observed as compound-nucleus resonances in proton elastic scattering and (p,n) reactions have been studied using the target isotopes Mo^{92}, Mo^{94}, Mo^{95}, Mo^{96}, Mo^{97}, Mo^{98}, and Mo^{100}. The observed resonances which occur at high excitations in the target-plus-proton system have been analyzed using a Coulomb-plus-single-level formula. The spectroscopic information for these resonances is compared with the analogue states in the target-plus-neutron system as observed in (d,p) reactions on the same targets. Level separations, l-value determinations and corresponding spectroscopic factors show remarkable agreement with the (d,p) data. A survey of the experimentally determined Coulomb displacement energies (ΔE_c) has been performed via the relation $\Delta E_c=C\,Z/A^{1/3}$. It is found that C is fairly constant for all the molybdenum isotopes.

1. INTRODUCTION

RECENTLY, the existence of isobaric analogue states at very high excitations in heavy nuclei was verified by observing them as compound-nucleus resonances.[1,2] A detailed description[3] of isobaric analogue resonances has shown that their existence can be understood within the framework that has been used to explain the occurrence of isobaric analogue states formed by the (p,n) charge-exchange mechanism.[4] Consequently, the existence of analogue states as compound states is to be expected in all nuclei.

Because of the simple relation between states belonging to the same isobaric spin multiplet, it follows that there is also a simple relation between the resonances observed in proton-induced reactions and the corresponding states seen in neutron capture via (d,p) stripping on the same target nucleus. Information gained by observing analogue resonances in proton-induced reactions is essentially equivalent to the information gained from (d,p) stripping, so that proton reactions via analogue states constitute an alternative method for nuclear-spectroscopic studies.

The present paper is the first of a series of papers in which the possibility of using analogue-state resonances as a tool in nuclear spectroscopy is exploited. The experimental results obtained here for the seven molybdenum target isotopes Mo^{92}, Mo^{94}, Mo^{95}, Mo^{96}, Mo^{97}, Mo^{98}, and Mo^{100} concern the resonances in the corresponding technetium isotopes produced as compound systems in proton-induced reactions. This study yields information on the spins and parities of the low-lying states of the Mo isotopes belonging to the same isobaric multiplets as the resonances in the compound system. A comparison between the present results and the available (d,p) data illustrates how powerful a technique the analogue-state method of studying nuclear spectra can be in practice.

The observations of analogue-state resonances provide a measure of Coulomb energy which is more accurate than previous methods of measuring this quantity. The systematics of Coulomb energies for the Mo isotopes are discussed in Sec. 4.

2. THEORY

Elastic scattering of protons through nuclear states can be a useful means for measuring the properties of

* Supported in part by the U. S. Air Force Office Scientific Research and U. S. Office of Naval Research.
† Present address: Physics Department, University of Texas, Austin, Texas.
‡ Present address: Physics Department, University of Washington, Seattle, Washington.
§ Present address: Physics Department, University of Florida, Gainesville, Florida.
[1] J. D. Fox, C. F. Moore, and D. Robson, Phys. Rev. Letters **12**, 198 (1964).
[2] L. L. Lee, Jr., A. Marinov, and J. P. Schiffer, Phys. Letters **8**, 352 (1964).
[3] D. Robson, Phys. Rev. **137**, B535 (1965).
[4] A. M. Lane, Nucl. Phys. **35**, 676 (1962).

nuclear levels. In nuclei having widely separated levels, the analysis is simplified in that only one level need be considered at a time. For this reason, resonance theory has been applied to elastic-scattering measurements in light nuclei at low excitation energies.

In heavy nuclei at high excitation energies, the nuclear energy levels are usually treated as a continuum. The elastic-scattering cross section is consequently analyzed on the basis of the complex potential-well model. Isobaric analogue resonances can occur in this same energy region but may stand out from the continuum because they have relatively large proton reduced widths, but small observed widths due to the Coulomb barrier.

One of the distinct advantages of studying nuclear spectra by elastic scattering as opposed to measuring the angular distributions of the proton groups formed in (d,p), reactions is the relative independence of the elastic-scattering interpretation on the reaction mechanism assumed. Although distorted-wave Born approximation calculations indicate that (d,p) reactions have angular distributions that are dependent on Q value and the orbital angular momentum of the captured proton, the angular distributions are not unambiguous and are sensitive to the parameters used in describing the (d,p) reaction mechanism. The Coulomb-resonance interference pattern that is characteristic of charged-particle elastic scattering, on the other hand, is quite independent of assumptions about reaction mechanism or nuclear properties.

In this work, the proton elastic-scattering resonances which we identify as isobaric analogue states are to be compared with their "neutron analogues," the states of the same isobaric spin multiplet that are formed as final states in the (d,p) reaction using the same target nuclide. The orbital angular momenta of the proton added to form the compound system and the neutron added in the (d,p) reaction are the same if the states are isobaric analogues. If T is a good quantum number, the reduced widths of the isobaric analogue states are related by

$$\gamma_p^2=[1/(2T_0+1)]\gamma_n^2, \tag{1}$$

where $T_0=T_z$ is the isobaric spin of the target, γ_p^2 is the reduced proton width of the "proton analogue," and γ_n^2 is the reduced neutron width of the "neutron analogue" which would be formed via a (d,p) reaction.

The (p,n) reaction data are not as amenable to careful analysis as the elastic-scattering data. It is useful, however, to provide a check on the positions of resonances when they are close together and the elastic-scattering analysis becomes complicated. In addition, it is possible to detect analogue resonances in the (p,n) reaction for lower proton energies than is the case for proton elastic scattering. The (p,n) data may also be necessary for a complete analysis of the partial widths of the analogue resonances.

The behavior of proton elastic scattering has been formulated in many general theories,[5,6] all of which give essentially the same results. The shape of the excitation curve near a single level in the compound system is almost completely characterized by the orbital angular momentum of the captured proton. The extraction of the other resonance parameters (e.g., J^π—spin and parity, E_J—resonance energy, Γ^J—total state width, and $\Gamma_{sl}{}^J$—partial width) can be estimated by inspection but a detailed evaluation requires a calculation of the elastic-scattering cross section. The differential elastic-scattering cross section is given by

$$\frac{d\sigma}{d\Omega}=\left(\frac{d\sigma}{d\Omega}\right)_{\text{Coulomb}}+\left(\frac{d\sigma}{d\Omega}\right)_{\text{interference}}+\left(\frac{d\sigma}{d\Omega}\right)_{\text{resonance}}, \tag{2}$$

$$\left(\frac{d\sigma}{d\Omega}\right)_{\text{Coulomb}}=\frac{\pi}{k^2}|C(\theta)|^2, \tag{3}$$

$$\left(\frac{d\sigma}{d\Omega}\right)_{\text{interference}}=\frac{1}{(2I_1+1)(2I_2+1)}\frac{\sqrt{\pi}}{k^2}\sum_{slJ}(2J+1)\times\mathrm{Re}[iT^J{}_{SlSl}C(\theta)]P_l(\cos\theta), \tag{4}$$

$$\left(\frac{d\sigma}{d\Omega}\right)_{\text{resonance}}=\frac{1}{(2I_1+1)(2I_2+1)}\frac{1}{k^2}\sum_{SS'K}B_K(S,S')\times P_K(\cos\theta), \tag{5}$$

where

$$B_K(S,S')=\tfrac{1}{4}\sum_{\substack{J_mJ_n\\ l_ml_m'\\ l_nl_n'}}(-1)^{S-S'}\bar{Z}(l_mJ_ml_nJ_n;SK)\times l\bar{Z}(_m'J_ml_n'J_n,S'K)\times T^{J_m}{}_{Sl_mS'l_m'}T^{J_n*}{}_{Sl_nS'l_n'}, \tag{6}$$

$$T^J{}_{SlS'l'}=e^{2i\omega_l}\delta_{ll'}\delta_{SS'}-[e^{i(\omega_l-\varphi_l)}e^{i(\omega_{l'}-\varphi_{l'})}]\times\left\{\delta_{SS'}\delta_{ll'}+\frac{i\sqrt{(\Gamma^J{}_{Sl})}\sqrt{(\Gamma^J{}_{S'l'})}}{(E_J-E)-\frac{1}{2}i\Gamma^J}\right\}, \tag{7}$$

$$C(\theta)=\frac{1}{2\sqrt{\pi}}\eta\csc^2(\theta/2)e^{-2i\eta\ \ln\sin(\theta/2)}$$

$$k^2=4.7848ME\ (\mathrm{b})^{-1},$$

$$\eta=0.157480Z_IZ_T(M/E)^{1/2},$$

$$\omega_l=\sum_{m=1}^{l}\arctan(\eta/m),$$

[5] A. M. Lane and R. G. Thomas, Rev. Mod. Phys. **30**, 257 (1958).

[6] H. Feshbach, Ann. Phys. (N. Y.) **5**, 357 (1958); J. Humblet and L. Rosenfeld, Nucl. Phys. **26**, 529 (1961).

with

$$|I_1-I_2| \leqslant S \leqslant I_1+I_2,$$
$$|J-S| \leqslant l \leqslant J+S,$$
$$|J_n-J_m| \leqslant K \leqslant J_n+J_m,$$
$$|l_n-l_m| \leqslant K \leqslant l_n+l_m.$$

In these equations J^π are the resonance level spins, I_1 and I_2 are the projectile and target spins, S is the channel spin, l is the orbital angular momentum, and ϕ_l is the phase shift for the lth partial wave due to nuclear potential scattering. M is the reduced mass in units of amu and E is the relative center-of-mass energy in MeV.

These formulas have been derived from R-matrix theory.[5] Since the observed levels are well below the Coulomb barrier the effect due to nuclear potential scattering is expected to be small. The formulas are based on the assumption that the resonance is due to an isolated level of the compound nucleus or to a single giant resonance. This giant resonance aspect of isobaric states is discussed by Robson.[3] In contrast to stripping reactions this analysis does not rely on a detailed model for the nuclear reaction mechanism.

The size of the resonance in the elastic scattering cross section is primarily determined by Coulomb-resonance interference. This interference is dependent to a large extent upon the simple factor $(2J+1)\Gamma_{sl}{}^J/(2I_1+1)(2I_2+1)\Gamma^J$. Large elastic-scattering resonances are therefore expected when the spin of the target is zero and competing neutron emission is forbidden.

Equations (2) through (11) have been programmed for the IBM–709 computer for the special case of spin-$\frac{1}{2}$ particles scattering from spin-zero targets ($J_t=0$). The program uses a nonlinear least-squares fitting routine which searches for the best values of the resonance parameters E_J, $\Gamma_{sl}{}^J$, Γ^J, and ϕ_l. This program fits one angle at a time. The l values are chosen by inspection, whereas the J^π values, which cannot be determined from the fits, are chosen either from values used in (d,p) studies or from shell model considerations. Figure 1 indicates a theoretical fit at three angles to the striking s-wave resonance in the reaction $Mo^{92}(p,p)$ with $\Gamma_l{}^J=12$ keV, $\Gamma^J=41$ keV, and $E_J=5.31$ MeV. In this case the target spin is zero and the neutron channels are closed.

The theoretical fits in this paper have all the on-resonance and off-resonance nuclear phase shifts put to zero since they are not expected to alter the size of the resonance parameters very much. These phases are very important, however, in measuring the deviations of the nonresonance cross section from the pure Coulomb cross section.[7] A program which fits resonances for any spin target and projectile is presently being developed which will also fit excitation functions at several angles at once. This should allow one to determine the nuclear phase shifts for several l values as well as determine the desired resonance parameters.

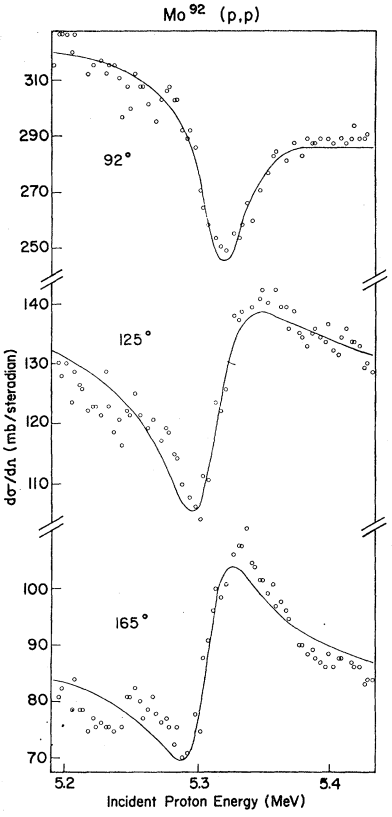

FIG. 1. s-wave fit to the $Mo^{92}(p,p)$ resonance with the best-fit parameter values of $E_{res}=5.31$ MeV, $\Gamma_p=12$ keV, $\Gamma=41$ keV, and $\phi_0=0$.

3. EXPERIMENT

The targets for this experiment were metal oxide layers on supporting carbon backings. The carbon foils were approximately 25 μg/sq cm thick and the target materials were from 100 to 200 μg thick as determined by Rutherford scattering. These thicknesses correspond to an energy loss of 0.5 keV at 5 MeV for the carbon and 1–3 keV for the target material.

A high-vacuum carbon-arc evaporation method was used to put the carbon backing onto a 1- by 3-in. glass microscope slide which was coated with a very thin film of detergent (Teepol) to facilitate separation of the carbon from the glass. At a back angle, elastic scattering was performed on a plain carbon backing. This foil revealed no impurities other than carbon and oxygen with an upper limit estimated to be one part in 5000 for heavy impurities.

Isotopically enriched[8] MoO_3 was evaporated onto the carbon-backed glass slides in high vacuum using an electron gun. The MoO_3 was placed in a carbon boat 0.05 in. in diameter which was supported on a tungsten rod and surrounded by a 0.030-in. tungsten wire shaped into a helix 0.25 in. in diameter. The carbon boat, held

[7] J. D. Fox, P. Richard, C. F. Moore, and D. Robson, Bull. Am. Phys. Soc. **10**, 496 (1965).

[8] Separated isotopes obtained from Oak Ridge National Laboratory.

at a positive potential, could be heated by electron bombardment from the hot filament which was near ground potential. The carbon sublimation temperature of[9] 3152°C is the limiting feature of this technique. In most instances for MoO_3 the radiant heat from the filament was enough to produce evaporation and the positive potential was not applied to the carbon boat.

The target foil was then floated off the glass slide onto ion-exchanged water prepared by passing distilled water through a de-ionization column. The foil was lifted off the water using aluminum target frames. Two types of frames were used; a rectangular frame ($\frac{5}{16}\times\frac{3}{8}$ in.) for elastic scattering and a circular frame ($\frac{3}{4}$-in. diam) for (p,n) reactions.

The proton-elastic-scattering work was done in a target chamber especially built for solid-state counters. The beam entrance slits were $\frac{1}{8}$ in. in diameter. The slit system defining the counter geometry consisted of a $\frac{1}{8}$-in.-diam collimator, 1.524 cm in front of a rear slit of $\frac{1}{16}$-in. diam placed just before the counter. The larger slit served only to stop particles whose source was other than the target. This slit was not intended to define the solid angle. The small slit was placed approximately 2.16 in. from the target. This resulted in a solid angle of 6.57×10^{-4} sr.

The scattered protons were detected using both surface-barrier and lithium-drifted solid-state counters. Three detectors, placed at 92°, 125°, and 165° to the incident beam were used. The resulting current pulses were amplified first by preamplifiers and then by DD2-type linear amplifiers. The voltage pulses were analyzed using two TMC 256-channel analyzers and one TMC 1024-channel analyzer.

The spectra showed proton groups from elastic scattering on oxygen and carbon as well as from the nucleus being studied. The three proton groups were easily distinguishable at angles greater than 90 deg. After examining the spectra for contaminants, the data were taken with the oxygen and carbon groups biased out of the analyzer to reduce the analyzer dead time.

The energy resolution for the detector system was 40–70 keV for an incident proton energy of 5 MeV.

Because the neutron background from collimating slits becomes excessive for proton energies greater than 7 MeV, the target chamber used for the (p,n) work was designed with no entrance slits. A quadrupole lens was used to focus the beam to a spot (usually smaller than $\frac{1}{4}$ in. in diameter). To minimize the background the beam was stopped 12 ft behind the target by a lead backstop.

The neutrons were detected in a Hanson-McKibben BF_3 long counter placed at 90 deg to the beam and 4 in. from the target. The pulses were preamplified and amplified in a Hamner Model N-302 amplifier. The neutron counts were recorded in a Hewlett-Packard scaler.

An incident proton beam was supplied by the tandem Van de Graaff accelerator at Florida State University. Our experiments required an energy range from 4 to 9 MeV. Beam energy spread was determined to be less than 1 keV by observing fine structure in the 9.25-MeV compound nucleus resonance in Tc^{93}.[10]

The beam current used for the elastic scattering was generally 1 μA focused through a $\frac{1}{8}$-in.-diam collimator. The beam used in the (p,n) work was not defined by a slit system beyond that following the 90° energy analyzer of the accelerator. This current ranged from 0.2 to 0.5 μA.

An integrated beam of the order of 100 μC was used for a single data point. Approximately 3 min was required to take each point, 1 min of which was the time required to print out and record the data. While printing out the data the accelerator was stepped in energy and readied for the next point.

A standard HVEC 90° magnet with nuclear magnetic resonance probe was used to analyze the beam energy. Energy calibration has been achieved by using the $C^{13}(p,n)$ threshold to determine the 90° magnet radius.

4. RESULTS AND CONCLUSIONS

A few remarks should be made concerning the general characteristics of the spectroscopic results. These comments are in regard to the trends which limit the energy range for useful data. Table I exhibits certain features of the data which will be referred to in the following discussion.

Considering only data for the proton analogue nucleus formed when the target is an even isotope of molybdenum, elastic scattering on the lower mass number isotopes (i.e., Mo^{92}, Mo^{94}, Mo^{96}) has a larger energy range of data exhibiting compound nuclear structure compared to the data on the higher mass number isotopes (i.e., Mo^{98}, Mo^{100}). The data on these lower mass number nuclei have sharper resonances and, in general, larger resonance amplitudes.

For even isotopes the (p,n) threshold decreases as the mass number increases for a given proton number. Simultaneously, the neutron binding energy decreases when going from lighter to heavier nuclei of the same chemical element. Because the Coulomb energy is nearly the same for all the molybdenum isotopes, the excitation energy for the ground-state isobaric analogue effectively increases relative to the threshold for neutron emission as A increases.

Another property to consider is the incident proton energy required to produce the isobaric analogue resonance. If this energy is far below the Coulomb barrier the proton penetrability is too small to produce a resonance with appreciable proton width. This, combined with the limited experimental resolution, causes the resonance amplitude to be insufficient to identify

[9] *Handbook of Chemistry and Physics* (Chemical Rubber Publishing Company, Cleveland, Ohio, 1964), 44th ed.

[10] P. Richard, C. F. Moore, D. Robson, and J. D. Fox, Phys. Rev. Letters **13**, 343 (1964).

TABLE I. Some of the relative variations encountered in the study of the isobaric states produced by proton bombardment on the even isotopes of Mo. Energies are given in MeV.

Target nucleus	Mo^{92}	Mo^{94}	Mo^{96}	Mo^{98}	Mo^{100}
(p,n) threshold[a]	9.08	5.05	3.72	1.5	1.1
E_p^{lab}, ground state	(4.36)	4.96	5.38	6.14	6.62
E_p^{lab}, $3s_{1/2}$ resonance[b]	5.31	5.74	6.06	6.14	6.62
B_n, neutron binding[c]	7.936±0.065	7.373±0.005	6.828±0.004	5.91±0.02	5.38±0.02
B_p, proton binding[a]	3.99	4.93	5.94	8.54	7.6
ΔE_c, Coulomb displacement energy	12.38±0.03	12.28±0.030	12.16±0.03	11.98±0.03	11.93±0.3
$C=\Delta E_c/(Z/A^{1/3})$	1.335±0.003	1.334±0.003	1.330±0.003	1.320±0.003	1.323±0.003

[a] *Nuclear Data Sheets*, compiled by K. Way *et al.* (Printing and Publishing Office, National Academy of Sciences—National Research Council, Washington 25, D. C., 1960), except for $Mo^{92}(p,n)$ threshold energy.
[b] The energy given here is that of the strongest s-wave resonance.
[c] R. R. Ries *et al.*, Phys. Rev. 132, 1673 (1963). [The binding energies obtained from (d,p) reactions, B. Cohen *et al.*, Phys. Rev. 135, B383 (1964), are in disagreement with the above numbers only for Mo^{92}.]

structure from the elastic-scattering data. An example of this sort of problem occurs in the study of $Mo^{92}+p$. The elastic-scattering data on Mo^{92} have not exhibited an observable resonance for the ground-state analogue of Mo^{93} at the expected proton energy of 4.36 MeV. In this case, the (p,n) threshold (9.08 MeV) is much higher than this resonance energy.

Since neutron penetrabilities tend to be large and are unaffected by the Coulomb barrier, (p,n) reactions provide a sensitive means for the identification of resonances so long as the proton bombarding energy is above the (p,n) threshold. The (p,n) cross section is usually sufficiently large to identify resonances in spite of the fact that neutron emission can occur only through isobaric spin admixtures in either the compound system or the final nuclear state. For the odd isotopes of molybdenum the proton energy required to produce the resonances corresponding to the low-lying isobaric states is well below the Coulomb barrier. The large ground-state spins of the odd isotopes ($\frac{5}{2}$) further diminishes the resonance amplitudes. However, the problem of measuring the energies of these nuclear levels is solved through use of the more sensitive (p,n) reaction.

The remainder of this section consists of detailed discussions of the spectra of isobaric analogue states produced by proton bombardment of the seven isotopes of molybdenum. A comparison will be made with the isobaric analogue states found here and the recent (d,p) results of Hjorth and Cohen[11] on the same targets.

Mo^{93}–Tc^{93}

The elastic-scattering data with a Mo^{92} target (91% Mo^{92}) is shown in Fig. 2. The resonances which have been analyzed in detail are indicated by arrows in the figure. The large s-wave resonance at 5.31 MeV is the

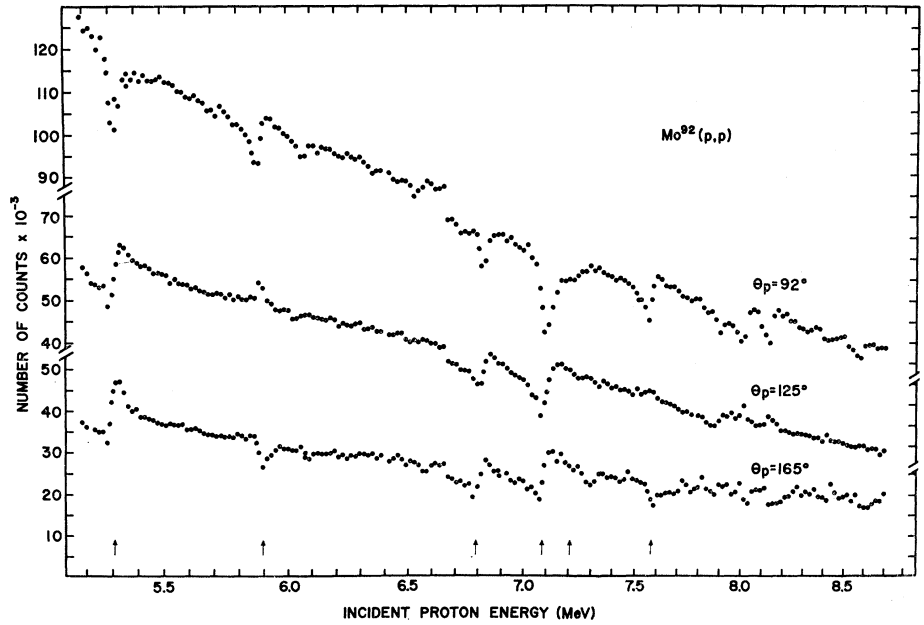

FIG. 2. Mo^{92} proton elastic-scattering data at three angles exhibiting analogue resonances. Arrows indicate resonances that have been analyzed.

[11] S. A. Hjorth and B. L. Cohen, Phys. Rev. 135, B920 (1964).

TABLE II. Elastic-scattering parameters for Tc^{93} levels and comparison to Mo^{93} levels.

$Mo^{92}(p,p)$						$Mo^{92}(d,p)$			
E_{res}^{lab} (MeV)	$E_p^{c.m.}-4.32$ (MeV)	Γ_p (keV)	Γ (keV)	l_p	S_{pp}	J^π	E_{ex} (MeV)	l_n	S_{dp}
(4.36)	...	...	...	...	...	$\frac{5}{2}+$	0.	2	0.87
5.31	0.93	12	41	0	0.60	$\frac{1}{2}+$	0.944	0	0.70
5.89	1.51	3	27	2	0.25	$\frac{3}{2}+$	1.486	2	0.43
...	...	...	...	...	...	$\frac{5}{2}+$	1.695	2	0.074
...	...	...	...	...	...	$\frac{3}{2}+$	2.186	(2)	0.083
...	...	...	...	...	...	$\frac{7}{2}+$	2.300	4	0.37
6.82	2.44	7	37	0	0.14	$\frac{1}{2}+$	2.445	0	0.15
7.18	2.78	16	49	0	0.26	$\frac{1}{2}+$	2.700	0	0.30
7.34	2.94	(3)	30	2	0.09	$\frac{3}{2}+$	2.850	2	0.087
7.57	3.17	5	40	2	0.10	$\frac{3}{2}+$	3.155	2	0.15
...	...	...	...	...	...	$\frac{3}{2}+$	3.426	2	0.13
7.98	3.58	...	...	(0)	...	$\frac{3}{2}+$	3.586	2	0.10
8.10	3.70	...	...	(2)	...	$\frac{3}{2}+$	3.693	2	0.083
8.22	3.82	...	...	(2)	...				
8.51	4.11	...	...	(0)	...				

isobaric analogue of the first excited state of Tc^{93} at 0.944 MeV. The isobaric analogue of the Tc^{93} ground state is expected to be at 4.36-MeV proton energy and was not identified in this experiment because of the low proton energy. Because the $Mo^{92}(p,n)$ threshold is at 9.08 MeV, this reaction could not be used for the identification of any of the isobaric analogue resonances investigated in this experiment.

The resonance parameters for the Tc^{93} resonance states which were analyzed according to Eq. (2) are given in Table II. Also included in the table are the energies and l_n values for the isobaric analogue levels in Mo^{93} as determined by (d,p) reaction data.

The value of S_{pp} for each resonance is also listed. S_{pp} is effectively a spectroscopic factor for the resonance found by taking the ratio of the "partial" spreading width (calculated in this case using the statistical model) to the observed spreading width $(\Gamma-\Gamma_p)$ as discussed in the Appendix. S_{pp} approximately indicates the single-particle strength of the resonance. It may be compared to S_{dp} which is the spectroscopic factor of the analogue state with $T=T_z$ determined by means of an analysis, using the distorted-wave Born approximation, of the (d,p) reaction populating the state.

Since Mo^{92} has a closed shell of 50 neutrons, the level structure of Mo^{93} can be expected to be very similar to that of Sr^{89} and Zr^{91}. The lowest shells have been found to be $2d_{5/2}$, $3s_{1/2}$, $3d_{3/2}$, and $1g_{7/2}$. The resonance states in Tc^{93} observed agree with this prediction except that we have no evidence for the $1g_{7/2}$ state observed in the (d,p) study of Mo^{93} at 2.300 MeV. Our data, however, could not rule this state out.

It should be noted here that the large s-wave reso-

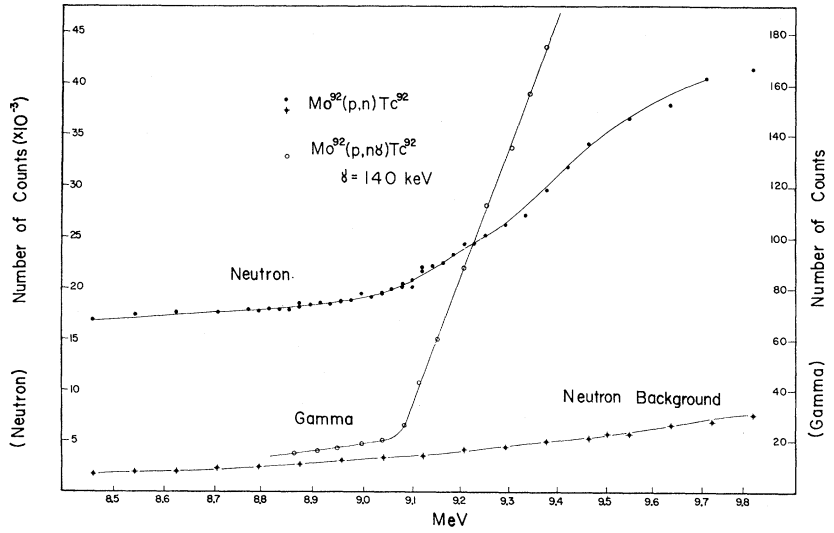

FIG. 3. Neutron threshold determination for $Mo^{92}+p$.

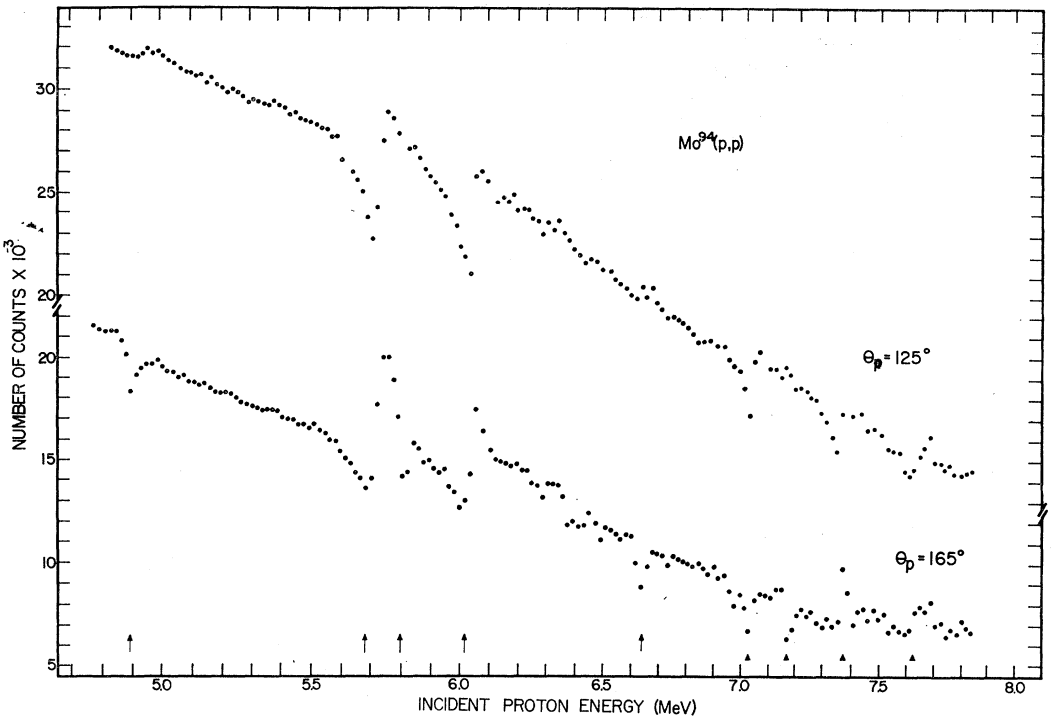

FIG. 4. Proton elastic scattering from Mo^{94} exhibiting analogue resonances in Tc^{95}.

nance at 5.31 MeV and the *d*-wave resonance at 5.89 MeV were the subject of a more careful investigation of the fine structure within the resonance. The details of this experiment and the analysis have been previously published.[3,10]

Incidental to this study of proton reactions and scattering, we have measured the threshold for the reaction $Mo^{92}(p,n)Tc^{92}$. The various gamma rays (140, 790, 1540 keV) from the decay of 4-min Tc^{92} could be detected. Neutrons were also detected but the neutron excitation function exhibited a rather insignificant discontinuity at threshold. This was caused by the high neutron background present in the experimental arrangement at the relatively high proton energies. The excitation functions of both the 140 keV gamma ray and neutrons are shown in Fig. 3. The excitation functions for the other gamma rays are similar and have the same threshold energy. We find that the (p,n) threshold is 9.08 ± 0.05 MeV. This threshold is about 300 keV higher than would be the case if the ground state of Tc^{92} were being produced at the kinematic threshold energy.[12] Since the spin of the 4-min ground state of Tc^{92} is 8 or 9, it is unlikely that we are producing this state directly near threshold. Our results imply that there is an excited state of Tc^{92} with more favorable spin within 300 keV of the ground state and that we have observed the threshold for the (p,n) reaction to this state.

[12] R. Van Lieshout, S. Monaro, G. B. Vingiani, and H. Morrinaga, Phys. Letters **9**, 164 (1964).

Mo^{95}–Tc^{95}

The elastic-scattering data for the Mo^{94} target (88% Mo^{94}) is shown in Fig. 4. Although there is evidence for considerable structure in the elastic-scattering cross section, especially above 6-MeV proton energy, only the resonances indicated have been analyzed in detail. In this case, the *d*-wave ground-state analogue is seen at 4.96-MeV proton energy. The isobaric analogue of the "first excited state" at 0.806 MeV which was identified in the (d,p) reaction study of Hjorth and Cohen[11] as being produced by a mixture of *d*- and *s*-wave neutrons is seen to be resolved into two components which are, in fact, *s*-wave and *d*-wave for the proton resonances. The theoretical fit to the *s*-wave state at 5.74-MeV proton energy and the *d*-wave state at 5.80-MeV proton energy are shown in Fig. 5. Hjorth and Cohen assigned the *d* wave to the lower of the two unresolved components, whereas the opposite is the case.

Although the proton-elastic-scattering data does not exclude them, the analogues of several levels, weakly excited in the (d,p) reaction, have not been identified. The resonance parameters for the elastic-scattering resonances that have been analyzed, and the comparison to the (d,p) results, are given in Table III.

It is worth noting that for the ground state of Mo^{95}, S_{dp} is 0.74 compared to the value of S_{pp} for the Mo^{95} analogue of 0.20. This represents the largest disagreement observed in these comparisons. Using optical-

model calculations rather than statistical-model calculations, one obtains a value of 0.18 for S_{pp}.

In order to check the energies of some of the isobaric analogue resonances found in the elastic-scattering data, the (p,n) excitation function was measured from below threshold to 7.5 MeV. These data are shown in Fig. 6. It is interesting to note that the small resonance at 4.96 MeV found in the (p,n) data is at the same energy as an elastic-scattering resonance even though this should be below the threshold for the (p,n) reaction. The observed strong break in the thin-target excitation function at 5.16 MeV corresponds very well with the beta-decay energy from the 52-min isomer (4367 keV) but the resonance at 4.96 MeV would imply the existence of a state in Tc^{94} even lower than the reported ground state.[13] The resonance cannot be due to impurities of the other isotopes of molybdenum. The thin carbon backing for the target is not responsible for this anomaly, although the data indicate a resonance near 4.0 MeV that could be assigned to carbon. We are continuing the study of this isotope in order to identify the origin of the 4.96 MeV anomaly in the (p,n) excitation function.

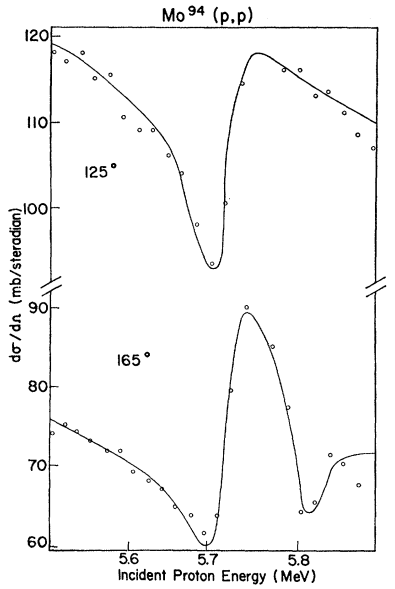

FIG. 5. Fits at two angles to the s-, d-wave doublet found in Tc^{95}.

Mo^{96}–Tc^{96}

The proton-elastic-scattering data shown in Fig. 7 were taken on a Mo^{95} target, enriched to 92%. Because the binding energy of a neutron to Mo^{95} is so large (9.158 MeV), the isobaric analogues of the Mo^{96} states fall at a relatively low proton bombarding energy. Elastic-scattering data were therefore not available for the ground-state analogue and for the analogues of the first few excited states. The energies of the resonances observed in the (p,n) reaction and in elastic scattering are tabulated in Table IV together with the excitation energies of the corresponding states observed in the (d,p) reaction.

No direct comparison with the (d,p) results can be made because there are no available angular distri-

TABLE III. Elastic-scattering parameters for Tc^{95} levels and comparison to Mo^{95} levels.

$Mo^{94}(p,p)$						$Mo^{94}(d,p)$			
E_{res}^{lab} (MeV)	$E_p^{c.m.}-4.91$ (MeV)	Γ_p (keV)	Γ (keV)	l_p	S_{pp}	J^π	E_{ex} (MeV)	l_n	S_{dp}
4.96	0.	0.6	18	2	0.20	$\frac{5}{2}^+$	0.	2	0.74
5.74	0.77	12	45	0	0.37	$\frac{3}{2}^+$	0.806	2	0.32
5.80	0.83	4	37	2	0.25	$\frac{1}{2}^+$	0.806	0	0.53
...	...	...	...	...	...	$\frac{5}{2}^+$	0.970	2	0.029
6.04	1.07	8	38	0	0.23	$\frac{1}{2}^+$	1.055	0	0.17
...	...	...	...	...	...	$\frac{1}{2}^+$	1.277	(0)	0.03
...	...	...	...	...	...	$\frac{5}{2}^+$	1.390	2	0.049
...	...	...	...	...	...		(1.478)		
6.61	1.58	2	26	2	0.09	$\frac{5}{2}^+$	1.630	2	0.11
...	...	...	...	...	...	$\frac{3}{2}^+$	1.80*	(2)	0.042
...	...	...	...	...	...	$\frac{1}{2}^+$	1.80*	(0)	0.025
...	...	...	...	...	...	$\frac{3}{2}^+$	1.95*	(2)	0.046
...	...	...	...	...	...	$\frac{7}{2}^+$	1.95*	(4)	0.44
7.01	2.04	5	20	0	0.18	$\frac{1}{2}^+$	2.08*	(0)	0.045
...	...	...	...	...	...	$\frac{3}{2}^+$	2.08*	(2)	0.25
7.13	2.14	3	31	2	0.09	$\frac{3}{2}^+$	2.172	2	0.14
...	...	...	...	...	...	$\frac{3}{2}^+$	2.275	(2)	0.094
7.35	2.37	1	10	(1)	0.06	$\frac{3}{2}^-$	2.39	(1)	0.098
...	...	...	...	...	...	$\frac{1}{2}^+$	2.52	(0), (1)	0.095
7.60	2.62	5	40	0	0.06	$\frac{3}{2}^-$	2.65	(2), (1)	0.12

[13] R. Van Lieshout (private communication).

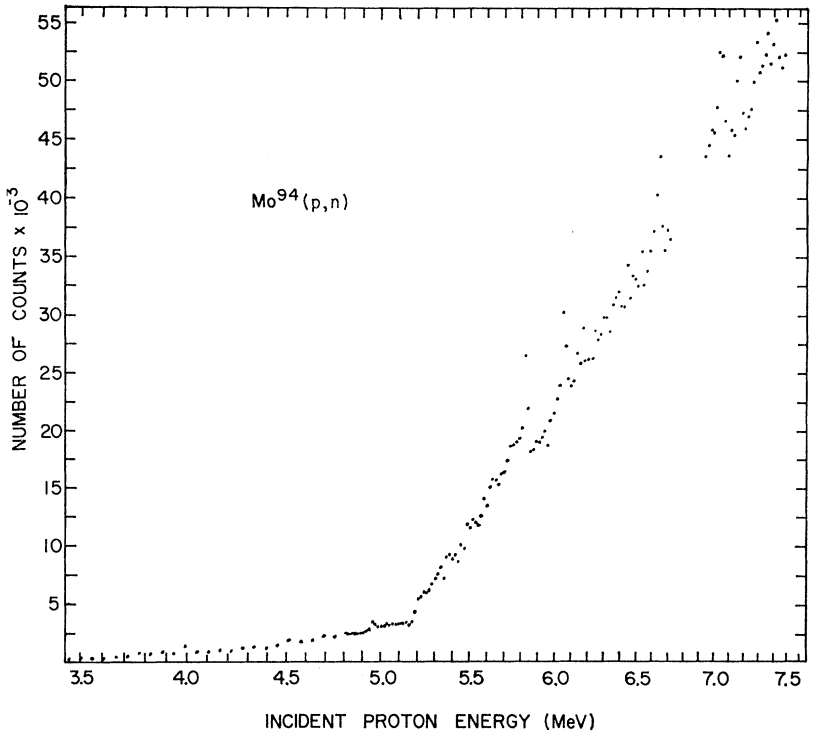

FIG. 6. (p,n) excitation function for Mo^{94}.

butions. In the region that was investigated by means of the (p,p) reaction, there are several resonances for which $l_p=0$ and 2. Because of the large number of states and the relatively high excitation in the analogue system, it is difficult to determine which of the levels excited in the (d,p) reaction are analogues of the proton elastic scattering resonances. The situation is further complicated by the fact that the spin of Mo^{95} is $\frac{5}{2}$ and the elastic scattering analysis is more difficult than for spin-zero targets.

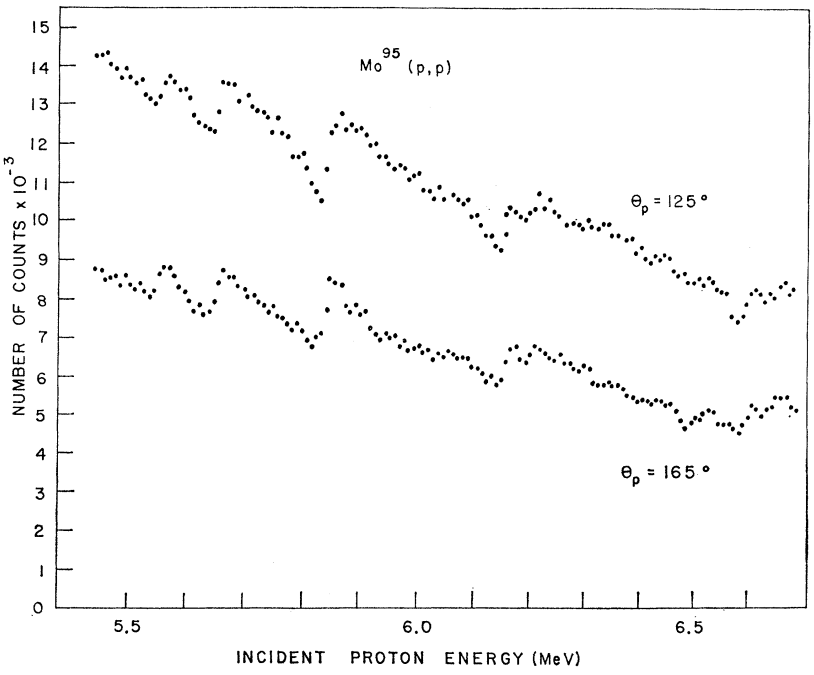

FIG. 7. Proton elastic scattering on Mo^{95}.

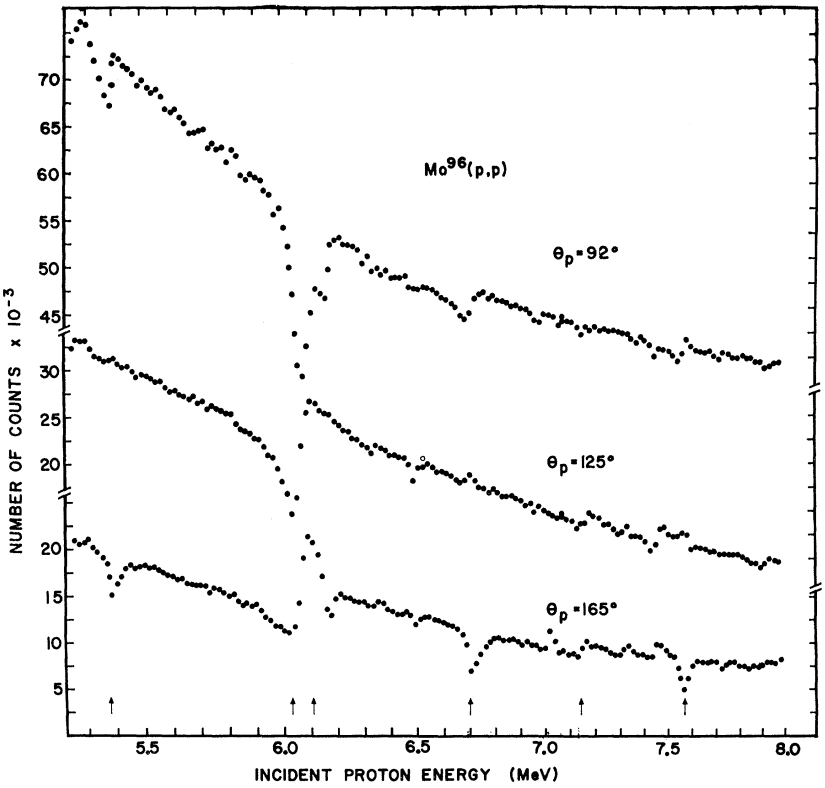

FIG. 8. Proton elastic scattering on Mo^{96}.

Mo^{97}–Tc^{97}

The elastic-scattering data taken with Mo^{96} targets, enriched to 91% Mo^{96}, are shown in Fig. 8. The ground-state analogue appears at 5.38 MeV and could easily be identified in the elastic-scattering data. Near 700-keV excitation in the analogue system, there is a well-resolved s- and d-wave doublet shown in Fig. 9. There was some structure reported at this energy by Hjorth and Cohen and they found it to be produced by $l=0$, 2, and 4 neutron capture. We are able to fit the elastic scattering data at this energy by assuming only two states formed by s- and d-wave proton capture. Other than

TABLE IV. (p,n) resonance energies in Tc^{96} and Tc^{98} and comparison to Mo^{96} and Mo^{98}.

$Mo^{95}(p,n)$ $E_p^{c.m.}-3.01$ (MeV)	$Mo^{95}(d,p)$ E_{ex} (MeV)	$Mo^{97}(p,n)$ $E_p^{c.m.}-3.48$ (MeV)	$Mo^{97}(d,p)$ E_{ex} (MeV)
0	0	0	0
0.85	0.78	0.76	0.74
1.25	1.15	0.82	0.79
1.64	1.64	1.45	1.44
1.91	1.88		1.52
2.08	1.99	1.77	1.77
2.15	2.10	2.24	2.28
2.32	2.23	2.34	2.34
2.50	2.43	2.56	2.58
2.59	2.55	2.67	2.63
2.70	2.71	2.77	2.73
	2.74	2.96	
		3.00	

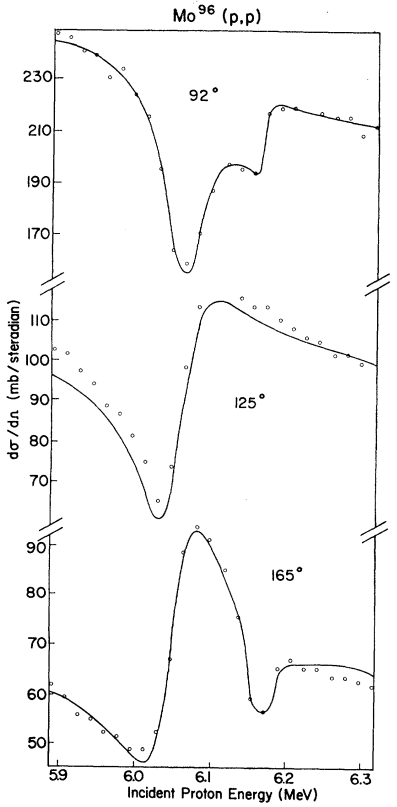

FIG. 9. s-, d-wave doublet analyzed in $Mo^{96}(p,p)$.

TABLE V. Elastic-scattering parameters for Tc^{97} levels and comparison to Mo^{97} levels.

$Mo^{96}(p,p)$							$Mo^{96}(d,p)$		
E_{res}^{lab} (MeV)	$E_p^{c.m.}-5.33$ (MeV)	Γ_p (keV)	Γ (keV)	l_p	S_{pp}	J^π	E_{ex} (MeV)	l_n	S_{dp}
5.38	0.	2.5	33	2	0.25	$\frac{5}{2}^+$	0	2	0.42
...	...	...	...	...	...	$\frac{7}{2}^+$	(0.699*)	(4)	1.28
6.06	0.67	31	68	0	0.68	$\frac{1}{2}^+$	0.699*	0	0.55
6.16	0.76	5	33	2	0.27	$\frac{3}{2}^+$	(0.699*)	(2)	0.28
6.47	1.07	...	...	(0)	...	$\frac{1}{2}^+$	0.893	0	0.11
6.71	1.31	10	57	2	0.22	$\frac{3}{2}^+$	1.271	2	0.34
...	...	...	...	...	...	$\frac{3}{2}^+$	1.450*	(2)	0.037
...	...	...	...	...	...	$\frac{7}{2}^+$	1.450*	(4)	0.30
7.03	1.63	(0.7)	(10)	(3)	0.03	$\frac{7}{2}^-$	1.554	3	0.22
...	...	...	...	...	...	$\frac{5}{2}^+$	1.70	(2)	0.024
7.17	1.77	...	...	(0)	...	$\frac{7}{2}^+$	1.78	(4)	0.24
7.32	1.92	...	...	(0)	...	$\frac{3}{2}^+$	1.96	2	0.030
7.44	2.04	...	...	(0)	...	$\frac{1}{2}^+$	2.065	0	0.15
7.56	2.16	7	35	2	0.16	$\frac{3}{2}^+$	2.153	2	0.22

this, the agreement with the (d,p) work of Hjorth and Cohen is quite good up to an excitation of about 1.5 MeV. Beyond this energy, the states become increasingly numerous and the data are very complicated. We miss several levels above 1.5 MeV that are weakly excited in the (d,p) reaction. However, the strong d-wave resonance near 7.6 MeV is undoubtedly the analogue of the $\frac{3}{2}^+$ level at 2.153 MeV which is produced very strongly in the (d,p) reaction. The fits to these data are summarized in Table V.

Mo^{98}–Tc^{98}

Elastic scattering on Mo^{97} yields the same inconclusive results as was obtained from Mo^{95}. The positions of resonances were obtained using the (p,n) reaction and a comparison with (d,p) excitation energies is made in Table IV.

Mo^{99}–Tc^{99}

The data obtained from the elastic scattering of protons from targets of Mo^{98} enriched to 90% are shown in Fig. 10. There are a great many resonances at low excitation energies and the analysis of those resonances above about 6.9 MeV proton energy is complicated by the necessity to consider more than one level at a time. The large s-wave resonance near 6.1 MeV is the isobaric analogue of the ground state of Mo^{99}. Theoretical fits to the ground state are shown in Fig. 11. The resonance that corresponds to an excitation of 0.60 MeV in the analogue system could not be fit as

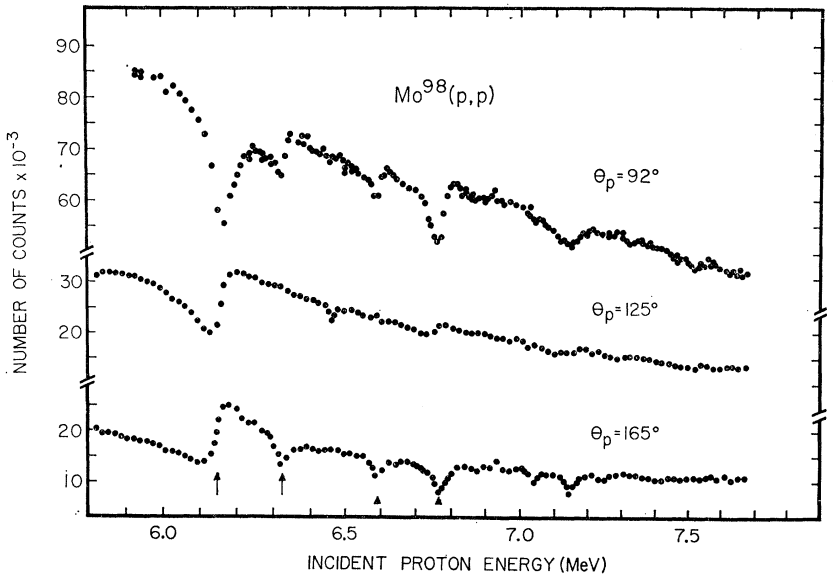

FIG. 10. Proton elastic scattering on Mo^{98}.

TABLE VI. Elastic-scattering parameters for Tc^{99} levels and comparison to Mo^{99} levels.

$Mo^{98}(p,p)$						$Mo^{98}(d,p)$			
E_{res}^{lab} (MeV)	$E_p^{c.m.}-6.08$ (MeV)	Γ_p (keV)	Γ (keV)	l_p	S_{pp}	J^π	E_{ex} (MeV)	l_n	S_{dp}
6.14	0.	29	68	0	0.56	$\frac{1}{2}^+$	0.	0	0.64
6.32	0.18	4	29	2	0.20	$\frac{5}{2}^+$	0.100	2	0.23
...	...	...	...	...	...	$\frac{7}{2}^+$	0.222	(3), (4)	0.42
6.58	0.44	(3)	(45)	(2)	0.08	$\frac{3}{2}^+$	0.361	2	0.10
...	...	...	...	...	...	$\frac{3}{2}^+$	0.545	2	0.35
6.74	0.60	(8)	(30)	(0)	0.21	$\frac{7}{2}^+$	0.644	(4), (5)	0.35
7.04	0.90	...	...	(0)	...	$\frac{3}{2}^+$	0.774	(2)	0.07
7.14	1.00	...	...	(2)	...	$\frac{3}{2}^+$	0.899	2	0.18

a single level and is probably an unresolved doublet produced by s- and d-wave protons.

The results of the fits and the comparison to the (d,p) work are shown in Table VI.

Mo^{101}–Tc^{101}

Four strong analogue resonances have been observed in Tc^{101}, as shown in Fig. 12, using a Mo^{100} target enriched to 86%. The ground state and first excited state have been observed and analyzed as a doublet as shown in Fig. 13. The $3s_{1/2}$ state is seen as the ground state in Mo^{99} as expected. It is also seen as the Mo^{101} ground state as discussed by Hjorth and Cohen.[11] In their (d,p) work on Mo^{100} the $3s_{1/2}$–$2d_{3/2}$ doublet is not resolved, whereas in the analogue experiment, the levels are clearly resolved. Table VII contains the comparisons.

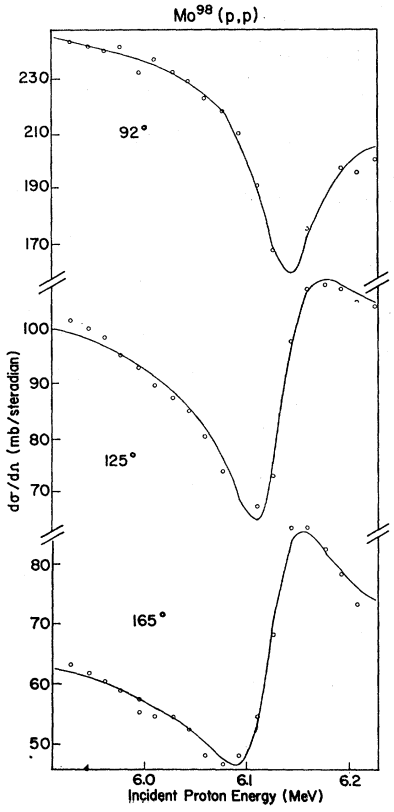

FIG. 11. s-wave fit to Tc^{99} resonance at 6.14 MeV.

Coulomb Displacement Energy

A by-product of the measurement of isobaric analogue resonance energies is the Coulomb displacement energy E_c. By this, we mean the Q value of a hypothetical (p,n) reaction between the isobaric analogue state with $T=T_z$ (the state formed by adding a neutron to the target), and the resonance formed by proton capture with $T=T_z+1$. The Coulomb displacement energies derived from our resonance measurements are given in Table I together with the parameter C obtained by dividing ΔE_c by $Z/A^{1/3}$. The Coulomb displacement energies for several nuclei have been measured by Anderson, Wong, and McClure[14] and our values for

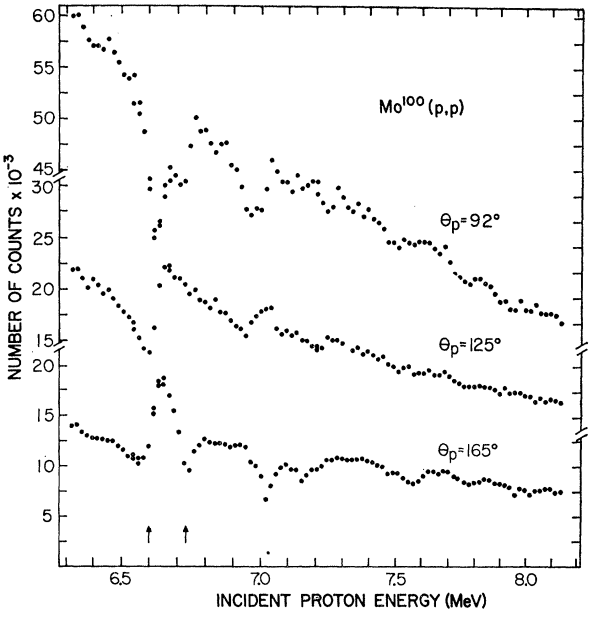

FIG. 12. Proton elastic scattering on Mo^{100}.

[14] J. D. Anderson, C. Wong, and J. W. McClure, Phys. Rev. 138, B615 (1965).

TABLE VII. Elastic-scattering parameters for Tc^{101} levels and comparison to Mo^{101} levels.

$Mo^{100}(p,p)$						$Mo^{100}(d,p)$			
E_{res}^{lab} (MeV)	$E_p^{c.m.}-6.55$ (MeV)	Γ_p (keV)	Γ (keV)	l_p	S_{pp}	J^π	E_{ex} (MeV)	l_n	S_{dp}
6.62	0.	30	73	0	0.41	$\frac{1}{2}^+$	0.*	0	0.42
6.73	0.09	9	45	2	0.24	$\frac{3}{2}^+$	0.06*	2	0.23
...	...	...	...	...	...	$\frac{7}{2}^+$	0.26*	4	0.52
6.98	0.36	...	...	(2)	...	$\frac{5}{2}^+$	0.32*	2	0.28
7.02	0.40	...	...	(2)	...	$\frac{3}{2}^+$	0.47*	2	0.11
...	...	...	...	...	...	...	0.53*	(1)	0.13

the molybdenum isotopes are in good agreement with theirs within the errors of the two measurements. The expected dependence of ΔE_c on A is verified by the constancy of C shown in Table I. However, additional measurements on other nuclides indicate that the relation is not as simple as that given here.

The determination of the Coulomb displacement energies by means of the isobaric analogue resonance technique affords approximately an order of magnitude better accuracy than the (p,n) time-of-flight technique used by Anderson, Wong, and McClure. It should be expected that the Coulomb displacement energy will show nuclear structure effects that are not consistent with the uniformly charged sphere model commonly used. This will be discussed in more detail in a subsequent article.

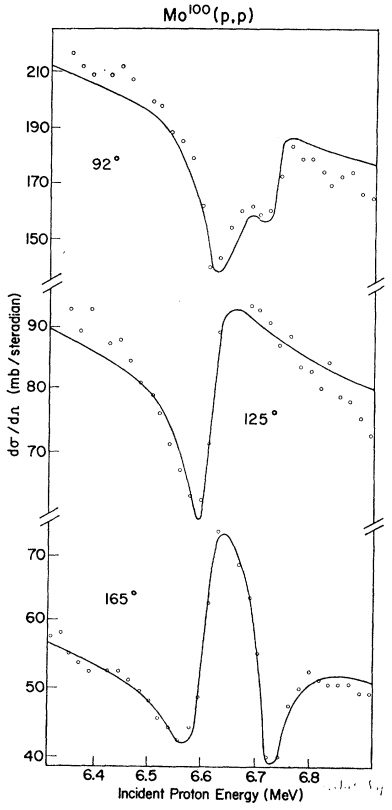

FIG. 13. s-, d-wave doublet analyzed in Tc^{101}.

5. SUMMARY

These results indicate that isobaric analogue states are very strong excited by proton reactions in medium-heavy nuclei, in many cases dominating the nuclear reaction cross section. The fact that the isobaric analogue states with $T=T_z+1$ do not mix strongly and do not disappear among the more dense $T=T_z$ states can be interpreted as an experimental verification of the idea of Lane and Soper[15] that relative isobaric spin is a good quantum number for heavy nuclei in the sense that the isobaric analogue states are states of relatively pure T spin. Accordingly, isobaric analogue states with $T=T_z+1$ decay by neutron emission only relatively weakly—through isobaric spin impurities in either the compound system or in the final state.

The investigation of Coulomb displacement energy systematics that we have begun here promises to give much more accurate Coulomb displacement energy results than obtainable by the method of Anderson, Wong, and McClure.[14] Careful fitting of theoretical shapes to the experiments allows this technique to give the resonance energy "E_p" to a relative accuracy of about 5 keV and an absolute accuracy of perhaps 10 keV. While the use of neutron separation energy data is necessary for the extraction of "ΔE_c" from our data, recent mass and reaction data can give this quantity to an absolute accuracy of about 10 keV.

Even though the errors in measuring the resonance energy is typically 0.2%, the errors in measuring Γ and Γ_p are typically 20%. The most sensitive parameter determined from the fits is Γ_p/Γ since this determines the magnitude of the interference term on resonance. This, therefore, means that the total error in calculating S_{pp}, which depends on $(\Gamma-\Gamma_p)$, is expected to be about 30%.

In addition to the nuclei discussed in this paper, extensive data have been taken on other nuclides and additional work will be undertaken to complete this study.

Preliminary evidence indicates that, for the very

[15] A. M. Lane and J. M. Soper, Phys. Rev. Letters 7, 420 (1961).

heavy nuclei, the isobaric analogue resonances are broadened almost to the point of unrecognizability. Investigation of the isobaric analogue resonances of much lighter nuclei is impaired by the fact that the analogues of the ground states occur below the proton separation energy. Where the excited states of the target plus neutron nucleus are well known, this experiment can be used in the identification of the excited-state analogues in light nuclei. A useful tool for investigating the bound-state analogues is the (He^3, d) reactions which can leave the residual nucleus (target+proton) in an analogue state of the target+neutron system.

ACKNOWLEDGMENTS

The authors wish to thank D. Burch, E. Estalote, S. I. Hayakawa, M. Himaya, D. D. Long, and G. Vourvopoulos for assistance in taking data. We also wish to thank the FSU Tandem Accelerator staff for attending to the problems of accelerator maintenance. We are grateful to the FSU Computing Center and the National Science Foundation for making computing time available for data analysis. The assistance of Mrs. T. Park in preliminary computer programming is appreciated.

APPENDIX: SPECTROSCOPIC FACTORS S_{pp}

For an analogue resonance formed by proton elastic scattering a spectroscopic factor S_{pp} may be defined by the relation

$$S_{pp}=\gamma_{\lambda p}^2/\sum_c \gamma_{\lambda c}^2, \tag{A1}$$

wherein $\gamma_{\lambda p}^2$ is the reduced width for the entrance channel and the sum over c involves only (proton +target) or (proton+target excited) channel configurations. A very similar spectroscopic factor S_{dp} is used in (d,ϕ) stripping reactions. Except for small differences due to the use of differently normalized radial wave functions we expect $S_{pp}\simeq S_{dp}$ for the corresponding analogue states observed in (p,ϕ) and (d,ϕ) reactions from the same target.

The spectroscopic factor S_{pp} is approximately related to the spreading widths $2W_\lambda^{(e)}$ introduced in Ref. 3. Using a statistical or optical model for the $T_<$ states we may use Eq. (4–12) of Ref. 3 and rewrite it in the more convenient form,

$$W_\lambda^{(e)}=\sum_c W_{\lambda c}^{(e)}, \tag{A2}$$

where the "partial" spreading widths are given by

$$W_{\lambda c}^{(e)}=b_c\gamma_{\lambda c}^2, \tag{A3}$$

$$b_c=\pi s_c|L_c^0|^2/g_c^2, \tag{A4}$$

and the quantities s_c, L_c^0, and g_c are defined in Ref. 3.

Because of the boundary conditions specified in Ref. 3, the sum over c in Eq. (A2) involves the same terms as those appearing in Eq. (A1), i.e., $L_c^0=0$ or $\gamma_{\lambda c}=0$ for all other channels. Calculations of the coefficients b_c for a variety of energies and partial waves show that b_c is *relatively* insensitive to the channel indices c *in comparison* with the variations of $\gamma_{\lambda c}^2$. Consequently, the entrance-channel coefficient b_p may be used to characterize the mean value of the b_c coefficient and we obtain the simple relation

$$S_{pp}\simeq[W_{\lambda p}^{(e)}]/[W_\lambda^{(e)}]. \tag{A5}$$

Useful estimates of S_{pp} may be obtained therefore when internal mixing is small, since we may substitute the *observed* spreading widths for the denominator in Eq. (A5). The entrance-channel spreading widths may be calculated from Eqs. (A3) and (A4) if a continuum or optical model is used to find the strength functions s_p.